# An Easy and User Independent Augmented Reality Based Navigation System for Radiation-Free Interventional Procedure*

Maria C. Palumbo, Laura Morchi, IEEE Member, Valentina Corbetta, Arianna Menciassi, IEEE Senior Member, Elena De Momi, IEEE Senior Member, Emiliano Votta, Alberto Redaelli

2022 International Symposium on Medical Robotics (ISMR) | 978-1-6654-6928-9/22/$31.00 ©2022 IEEE | DOI: 10.1109/ISMR48347.2022.9807461

***Abstract*— Despite offering numerous advantages, percutaneous treatments in interventional cardiology still present several limitations, including the recurrent use of fluoroscopy to track the route of the catheter during the intervention. In this study we propose an augmented reality (AR)-based navigation system for radiation-free interventional procedures using electromagnetic (EM) sensors. A customized tool embedding an EM sensor and a QRcode (automatically tracked in AR) was designed to perform the registration procedure. The accuracy of the system was assessed asking the user to evaluate the distance between the real position of the sensor and its holographic counterpart by means of a holographic measurement tool. Variability between intra- and inter-operator accuracy was assessed, each one performing 10 evaluation tests. Results showed a mean error of 2.70 ± 0.36 mm and 2.68 ± 0.79 mm for the intra- and inter-operator tests, respectively. To the best of our knowledge this is the first study that proposes a user independent procedure for calibrating an AR device with an EM system presenting a quantitative evaluation between intra- and inter-operators.**

## I. Introduction

Structural interventional cardiology (SIC) is the branch of interventional cardiology devoted to the percutaneous treatment of non-coronary heart diseases, i.e., the broad spectrum of congenital or acquired pathological conditions spanning from septal defects to heart valve diseases. In SIC procedures, a catheter is inserted from a peripheral access into a peripheral vessel, and subsequently driven through the bloodstream to the heart, where an implantable device is deployed to replace or to repair the diseased native structure targeted by the procedure.

Transcatheter technologies for SIC procedures have been a major breakthrough in the field, as they allowed for treating high-risk patients who wouldn't be eligible for classic open-chest surgery due to, e.g., old age or comorbidities [1]. Factors such as reduced complication rate, mortality rate, shorter length of in-hospital stay, while granting comparable outcomes with open surgery, make the percutaneous treatment of structural heart diseases cost-effective in different continents and healthcare systems [2], and in some cases even profitable to hospitals especially in high-volume centers [3].

Despite these advantages, SIC approaches are still affected by some limiting factors: i) lack of direct vision of the catheter and of the relevant anatomical structures make the use of 2D fluoroscopy required in every stage of the procedure; the repeated exposure of high doses X-ray leads to severe consequences for both operators [4] and patients, the latter aggravated by the use of nephrotoxic contrast agent to improve image quality; ii) anatomical complexity and dynamic behavior of the anatomical environment; iii) complexity of the proximal drivers that in some procedures prevent from clearly envisioning how operator's maneuvers at the proximal end will affect the distal end of the catheter.

For this reason, the ARTERY (Autonomous Robotics for transcatheter delivery systems) European project [5] aims at developing a novel radiation-free platform based on shared-autonomy robotic catheters for percutaneous procedures. The project will leverage on two fundamental pillars, Robotic Assisted Surgery (RAS) and Augmented Reality (AR). The catheter will be guided by an Artificial Intelligence (AI) module that will allow it to autonomously find its way towards the target. The operator will be able to monitor the progress of the catheter and, if needed, take control over the operation thanks to an AR environment that recreates the anatomy of the patient, as reconstructed from standard pre-procedural computed tomography (CT) scans, and the movement of the catheter.

Paramount to the success of this project is the development of a reliable method to i) track the catheter over the vessels and to ii) display it in the AR environment upon co-registration between the holographic environment and the physical counterpart. To this end, we present the proof-of-concept of a novel real-time navigation technique based on the capability of electromagnetic (EM) sensors to be tracked in space coupled with an AR head mounted display (HMD) to visualize the position of a sensorized catheter, avoiding the use of any radiation.

### A. State of the Art

Currently, only one commercially available robotic system resembles the functioning of ARTERY. That is the CorPath (Corindus, A Siemens Healthineers Company, Waltham, MA, USA) system. It is a remotely guided system mainly developed for Percutaneous Coronary Interventions (PCI). The operator drives the robot from an interventional cockpit, performing many steps of the endovascular procedures outside of the radiation field, yet it still relies on the use of fluoroscopy to monitor the catheter and does not avoid x-ray exposure of patients. A key advancement proposed by the ARTERY project is hence the use of AR to

*This work was supported in part by the ARTERY European project which has received funding from the European Union's Horizon 2020 research and innovation program under grant agreement No 101017140.

Corresponding author phone +39 02 2399 3370; Fax +39 02 2399 3360; e-mail: mariachiara.palumbo@polimi.it).

MC. Palumbo, V. Corbetta, E. De Momi, E. Votta, A. Redaelli are with the Department of Electronics, Information and Bioengineering, Politecnico di Milano, Milano, Italy.

L. Morchi, A. Menciassi are with the BioRobotics Institute and the Department of Excellence in Robotics & AI of Scuola Superiore Sant'Anna, Pisa, Italy.

facilitate the transition towards a truly radiation-free approach.

In the past decade, AR has seen an increased awareness in its powerful intraoperative guidance capability, as it allows to clearly visualize anatomical structures of interest, and to provide intraoperative information about the patient's anatomy or about the robot, by blending together different sources of information and displaying them simultaneously [6]. AR has already started to be applied in many different RAS procedures: through either *ad hoc* newly designed surgical setups or by previously existing setups supplemented with AR tools that provide improved information management with immersive user-interfaces in a surgical environment. For instance, AR have been proposed to provide direct view of the pose of the robotic instruments inside the patient body and a configurable visualization of the stereo endoscopy in robot-assisted laparoscopic surgery, using different fiducial markers [7]. Qian et al. proposed subsequently an autonomous control method for a flexible endoscope that tracks the surgeon's head position thanks to the AR HMD worn; the head-tracking is then used to capture images from the same perspective as the surgeon when the flexible endoscope is actuated. That solution allowed for the AR visualization of both the virtual frustum of the endoscope and its video projected directly on the patient [8]. To be able to accurately and safely exploit AR as a medium for Human-Robot Interaction in RAS, it is paramount to accurately register and track virtual objects in the real world. AR systems require highly capable head and object trackers to create an effective illusion of virtual objects coexisting with the real world. Currently, the state of the art is based on the use of fiducial markers to track the real objects of interest requesting however a constant line of sight. Technologies as EM sensors represent a viable alternative in the absence of a direct view, such as during endovascular procedures. EM tracking has indeed shown to provide effective assistance to surgeons or interventional radiologists during endovascular procedures performed in a surgical environment [9]. Additionally, solutions to avoid interferences due to the co-presence of the electromagnetic tracking hardware and X-ray technology, have been proposed by O' Donoghue et al. [10]. Of note, the system allows the usage of the EM technology to be applied to a wide range of different procedures where interference with the imaging modalities is a major concern.

Techniques to combine AR and EM sensors to monitor the movement of catheters and surgical instruments inside the patient with the purpose to reduce and eventually eliminate radiation exposure have already been investigated. In [11], Kuhlemann et al. present a real-time navigation framework that allows a 3D holographic view of the vascular system without any need of radiation. The patient's surface and vascular tree from pre-operative computed tomography data is registered to the patient using an EM tracking system. The AR environment is visualized via a HMD. Thanks to the EM tracking system, the framework also allows to display the position and orientation of a catheter. However, the efficacy of this methodology is hindered by the absence of a proper calibration technique for the 3D holographic overlay visualization and therefore it is not possible to evaluate the accuracy of the proposed approach. Similarly, Garcia-Vazquez et al. [12] presented a method for performing endovascular aortic repair (EVAR) combining a HoloLens1 HMD and an EM device and showed the feasibility of such a procedure without however presenting objective data endpoints nor quantitative results about the registration procedure.

A registration approach exploiting both a HMD and an EM tracking system has also been developed by Tu et al. [13] to support the distal interlocking of intramedullary nails. Despite the good accuracy reported by the authors, their calibration approach still relies on the operator's skills. Moreover, the described results only refer to the performance of one experienced user, thus the dependency of the registration procedure on the expertise of different operators remains an open question.

In the present study we propose a method comprehensive of a registration procedure to dynamically align the position of an EM sensor with a holographic marker and of an evaluation procedure to assess the accuracy of the previous step. Remarkably, the developed registration process is completely independent of human capabilities, and thus its performance is highly repeatable.

## II. Materials and Methods

### A. Hardware and Software Components

The ARTERY system involves four key hardware components (Fig. 1):

1. An EM tracking device (Aurora NDI, Aurora, Northern Digital Inc., Canada) consisting of its system control unit (SCU), system interface unit (SIU) with two 5 degrees-of-freedom (DoF) sensors;
2. A catheter guidewire whose tip embeds one of the two EM sensors so to allow for its real-time tracking;
3. A calibration tool embedding the second EM sensor and designed to identify the transformation allowing for registering the real EM position in the holographic 3D space;
4. A HoloLens2 (Microsoft Inc., USA) HMD to visualize the guidewire tip avatar in real time. This specific HMD was chosen because of its overall performance and design improvement with respect to the first version of the device that was already considered one of the most suitable HMD among other commercial devices for surgical applications [14].

Data transfer from the EM sensor to the HMD and registration are carried out by the EM sensor API and by a

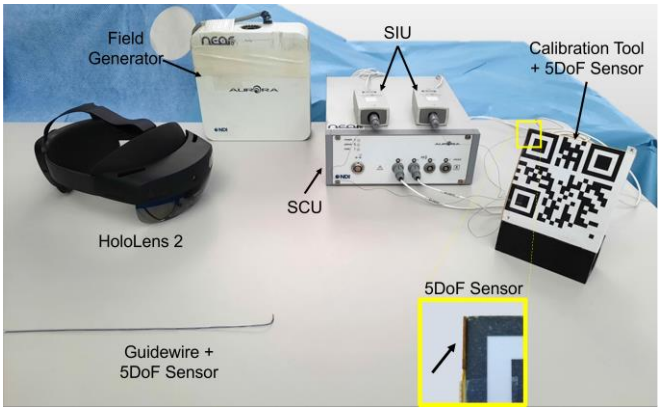


Fig. 1. Hardware components of the experimental setup: EM tracking device (Aurora NDI) consisting of its system control unit (SCU), system interface unit (SIU) with two 5DoF sensors embedded both in the calibration tool and in the guidewire, and HoloLens2 head mounted display.

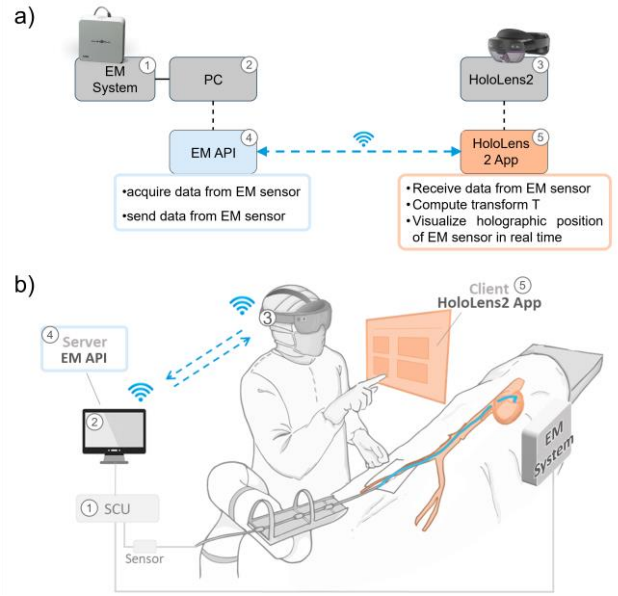


Fig. 2. System overview of the ARTERY catheter tracking system. a) flowchart describing the connection between hardware (in gray: (1) EM system, (2) computer to which (1) is connected, (3) HoloLens2 HMD) and digital components (in blue the (4) EM application programming interface API, (5) UWP HoloLens2 in orange); b) drawing showing the use of the proposed system in a possible clinical scenario.

dedicated holographic Universal Windows Platform (UWP) application, respectively (Fig. 2). The holographic UWP application was developed using the Unity3D development platform (Unity Technologies, version 2020.3.12LTS) together with the mixed reality toolkit library MRTKv2.5.3.

To access the position of the sensor from the PC where the EM system is connected, the scikit-surgerynditracker library was used [15]. This library implements a python interface for Northern Digital (NDI) trackers and is specifically designed to enable rapid development of clinical applications for image-guided interventions [15]. Data exchange between the application running on HoloLens2 and the python code retrieving the sensor data was ensured using a user datagram protocol (UDP). In this application, the host computer acts as the server containing the sensor data and HoloLens2 acts as the client requesting the sensor data from the host computer. The python script including the scikit-surgerynditracker library was slightly modified to integrate the software pipeline that makes the host computer a server capable of transmitting the sensor data upon request. Similarly, scripts using DatagramSocket were added in the HoloLens2 app to request and receive data from the server. Data from the EM system was delivered at an update rate of 40 Hz, while HoloLens2 app frequency was kept at least at 60 fps to ensure the best hologram quality and stability.

### *B. Calibration Procedure*

The core idea of the calibration procedure is to compute the registration matrix that superimposes the virtual marker on the physical EM sensor and to receive this transformed position at each frame in a continuous manner. Every virtual object rendered in the holographic scene is positioned with respect to a global left-hand coordinate system {G} computed from the HoloLens2 device when starting the application. This global coordinate system is stable and fixed while the application is running. The 5DoF sensor position on the other hand, is represented with respect to Aurora right-hand global coordinate system {A}, based on the field generator's characterized measurement volume (Fig. 3a). The measurement volume consists of a cubic region with a 50 cm edge length and point of origin in the field generator center. To register these two spaces and then achieve a calibration procedure, location of fiducial points whose coordinates are known in both spaces are required. For this reason, we implemented a system based on the capability of HoloLens2 to detect QRcodes in the environment around the headset, establishing a coordinate system at each code's real-world location. Fig. 3b shows the printed QRcode fixed on a rigid support and the holographic coordinate system appearing on the top left corner. To couple the position of the QRcode in the {G} coordinate system with the position of the sensor in the {A} coordinate system, the sensor was positioned and kept fixed during the overall calibration procedure on the rigid QRcode support (Fig. 3c), letting the two local coordinate system, one from the sensor and one from the QRcode detection, be aligned at their center.After starting the EM API running on PC and the HoloLens2 app, the user is required to move the QRcode sensorized tool in four different positions spanning the four edges of the EM acquisition volume. By design, this step requires no particular attention when positioning the panel: the user could choose four positions of his/her choice with different coordinates. However, in the present study these four positions were chosen once, prior to the experimental campaign, by evaluating the limits of the acquisition volume and were kept the same for all the tests, using the same supports on which to position the sensorized panel, so to make the results as comparable as possible. A detailed workflow description of this process is shown in Fig. 4. Actions that need to be done in the holographic app are represented in the orange blocks.

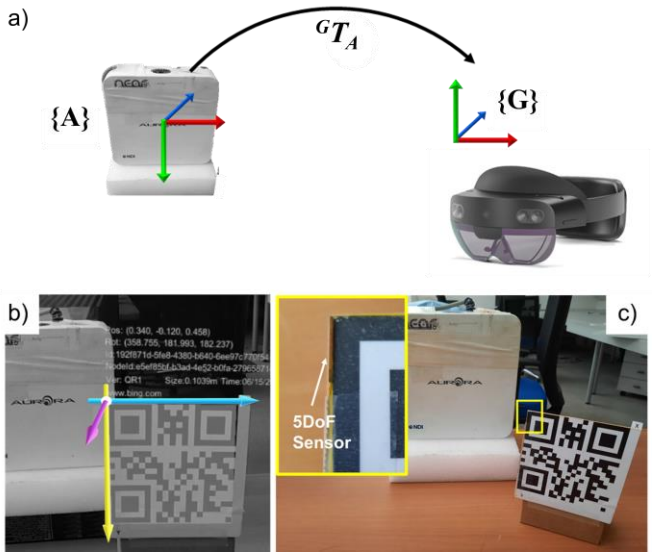


Fig. 3. Setup required for the registration procedure. a) Different coordinate systems between Aurora NDI {A} and HoloLens2 {G} and their transformation matrix ${}^{G}T_{A}$; b) holographic coordinate system automatically tracked on QRcode rigid panel, real image components are in greyscale modality, while AR components are in RGB modality. c) Rigid QRcode panel with embedded sensor used to physically align the position of the sensor with the detected hologram.

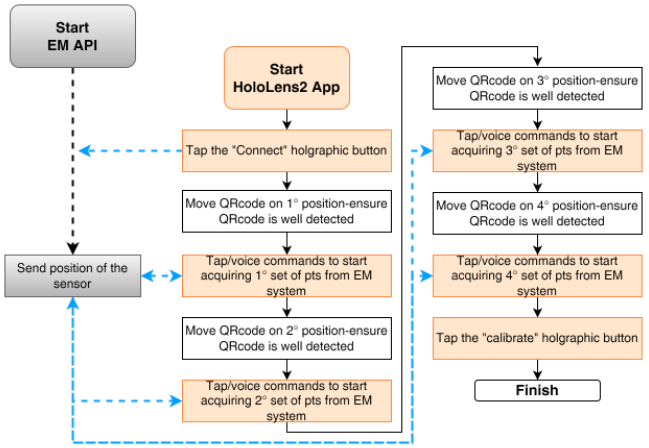


Fig. 4. Flow chart describing each step of the calibration procedure. Actions that need to be done in the holographic app are represented in the orange blocks, the EM API is represented in gray, while actions that need to be done by the operator are reported in white. Data exchange from the sensor to the App, and from the EM system to the EM API are represented with dotted blue and black lines respectively.

For each of the 4 positions, the user interacting with a holographic menu, sends a request to the server to receive the sensor's position while the tool is stationary. The tool is kept still for a few seconds until 10 sensor positions are received and averaged to cancel out possible noise from the sensor. Only one position was considered from the QRcode as no fluctuations were observed when the tracked object was still. The tool is then moved in different positions at different heights to have 4 complete different coordinates in the space from the sensor $p_i$ (i=1,…4), and from the QRcode $q_i$ (i=1,…4). (Fig. 5). After the 4 different positions are acquired, the two sets of corresponding 3D points are processed in the app to find the optimal rotation (R) and translation (T) matrix that aligns the positions received from the sensor in the {A} space to the {G} space. An algorithm to find the least-squares solution of R and T, which is based on the singular value decomposition (SVD) is applied to compute the registration matrix ${}^{G}T_{A}$ [16].

$$q_i = {}^{G}T_{A} \bullet p_i \tag{1}$$

To account for the change from right to left hand coordinate system the x-coordinate from {A} was considered as negative. Once the calibration procedure is performed, a virtual hologram dynamically matches its moving physical counterpart (the sensor's tip). Each time the deployed app is launched on HoloLens2, ${}^{G}T_{A}$ is unknown and unpredictable, and a new calibration procedure is required.

### C. Calibration Assessment

In this study we propose a new approach to assess the accuracy of the described calibration procedure. The accuracy evaluation when registering a hologram on a physical counterpart is considered a challenging task. This is because the hologram is only perceived from the user's eyes, letting the alignment between the virtual and real object only verifiable from the user himself. To measure the error between the position of the sensor tip and the hologram having the transformed sensor's position, we propose a method based on the localization of the physical tip of the sensor with respect to several holographic spheres of known size whose position in the space is given by (1). The radius of the sphere in which the sensor tip falls therefore corresponds to the error between the actual tip's position and the calculated position of the hologram. The layout is shown in Fig. 6a where six different spheres with a radius ranging from 1 mm to 6 mm were considered. When the error is close to 0 mm the center of these spheres is completely aligned with the sensor's tip while if the tip of the sensor falls in the sphere with a radius equal to 4 mm the error is considered to be 4 mm (Fig. 6b). In the proposed accuracy evaluation procedure, the user was asked to move the sensor in 9 different positions within the EM system acquisition volume and to assess in which of the six spheres the tip of the sensor was falling into, for each of the nine positions. These 9 positions are the same in each trial and correspond to the proximity of the 8 corners of the EM acquisition volume and 1 point at the center. Fig. 6c graphically shows the 9 positions in which the rigid panel with the attached sensor was moved during the evaluation procedure. While assessing its position with respect to the spheres, the panel with the attached sensor was kept still, placed on the table, and the user was free to move to better understand in which of the 3D spheres the tip was. In this part of the experiment the sensor was attached to a rigid support for comfort purposes, to prevent the user from introducing a physiological tremor when manually handling the sensor. An

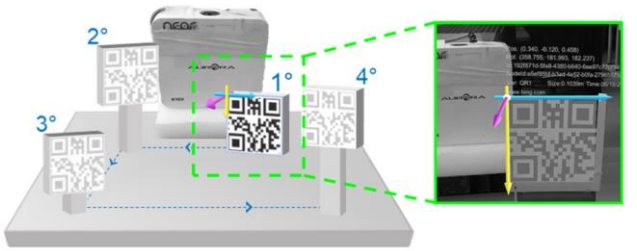


Fig. 5. Experimental procedure performed to calibrate the EM coordinate system and HoloLens2 coordinate system; real image components are in greyscale modality, while AR components are in RGB modality.

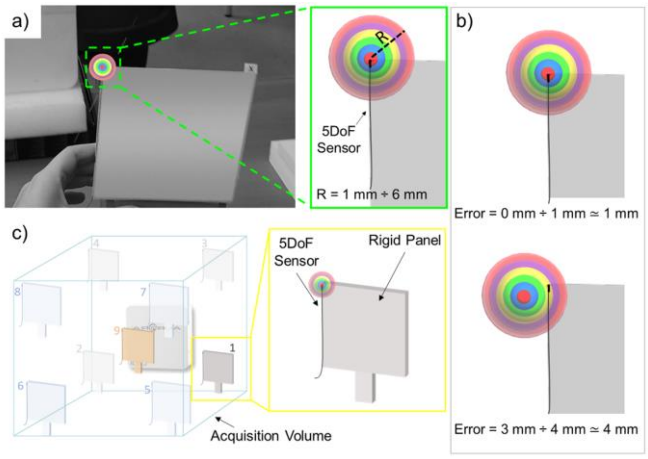


Fig. 6. Calibration assessment. a) colored holographic sphere with the transformed position from the sensor perfectly aligned with the sensor's tip, real image components are in greyscale modality, while AR components are in RGB modality; b) example of two possible evaluation situations; c) EM acquisition volume with the nine different positions in which the registration was evaluated. Rigid panel represented in gray, light blue or orange depending on the position with respect to the field generator (close, far, at the center).

intra- and inter-operator assessment was conducted for this study: we asked one experienced user to perform the calibration and evaluation procedure 10 times; while for the inter-operator assessment, 10 different non-expert users were enrolled to perform the calibration and evaluation procedure once. To make sure that holograms were correctly aligned, the "HoloLens2 eye calibration" was run for each user before the test. In every calibration procedure, the calibration error for each of the nine sensor positions was recorded, and the associated median value and interquartile range were computed for all the tests together with the frequency $n_e$ (e=1,...6) for each one of the considered values of error. This value is reported as a percentage $p_e$ of the total $N=6$ error values considered for all the tests carried out.

$$p_e = n_e / N, \quad e = 1, \ldots 6 \tag{2}$$

Statistical analysis was conducted using Matlab software (Mathworks, Massachusetts, United States). Within each case – namely, intra-operative and inter-operative – the frequencies of occurrence of the errors were compared with each other utilizing the $\chi^2$ test. In addition, the frequency of occurrence of each error was compared between the intra- and inter-operative case, by using the $\chi^2$ test. Three levels of statistical significance were used, i.e., P value < 0.05 (marked with '*'), P value < 0.01 (marked with '**') and P value < 0.001 (marked with '***').

## III. Results

To test the influence of the user's experience on the accuracy of the registration procedure, an intra- and inter-operator assessment was conducted for this study. Fig. 6a shows the holographic sphere perfectly overlapping the sensor's tip placed at the top left corner of the rigid support. The registration error among the intra-operator tests resulted in a global error of 2.70 ± 0.36 mm over all the evaluated points within the EM sensor acquisition volume. This means the tip of the sensor falls between the second and third colored sphere starting from the center, on average. Similarly, the inter-operator evaluation resulted in a global error of 2.68 ± 0.79 mm. Fig. 7 shows the median error for the 10 measurements done by a single operator and by multiple operators for each of the nine points in the acquisition volume.The position of the graph bars, with the associated median error, approximately respects the location in which the rigid support was placed within the acquisition volume. Fig. 8a shows the median and interquartile range over the nine points for each of the 10 tests done by a single and multiple operators, respectively referred to as "intra op" and "inter op". The percentage $p_e$ (e=1,...6) for each of the considered error values is shown in Fig. 8b and Fig. 8c. No statistically significant difference was found between each error of the intra-and inter-operative scenario (Fig. 8 b), thus showing that the method is effective independently from the expertise of the user accomplishing the procedure. A statistically significant difference can be appreciated in the frequency of occurrence of lower errors – namely, 1 mm and 2 mm – with respect to higher errors –namely errors greater than 4 mm – in both the intra-operative and the inter-operative case (Fig. 8c), thus confirming the accuracy of the proposed method. The registration time for the calibration procedure was 1.22 ± 0.05 minutes and 1.34 ± 0.08 minutes respectively for the single and multiple operator test.

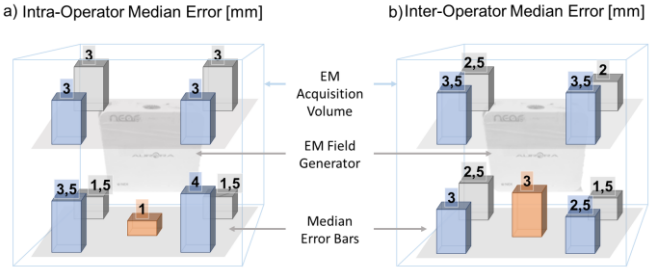


Fig. 7. EM field cubic acquisition volume with the nine different median errors in which the registration was evaluated for the a) 10 tests done by a single expert user and for the b) 10 tests done by multiple non-expert users. The EM field generator is represented on the back of the volume. Bars are color coded in gray, light blue or orange depending on the position with respect to the field generator (close, far, at the center).

## IV. Discussion

Minimally invasive interventions are rapidly replacing invasive surgical procedures for the most prevalent human disease conditions. Among these, percutaneous interventions are becoming an equally effective or even superior solution, as compared to standard open-chest surgery, to many non-coronary diseases, like aortic valve stenosis [17] and mitral valve regurgitation [18]. These procedures generally involve the insertion of a catheter into the femoral artery or into the femoral vein by an interventional physician, who threads the catheter under fluoroscopic guidance through the vasculature to the target cardiac structure. As a result, operators still rely on a significant use of fluoroscopy during all phases of the procedure remaining heavily exposed to x-ray together with the patient and echocardiographers in the specific context of interventional cardiology [19]. One of the main goals in the ARTERY project is indeed to eliminate the need for fluoroscopy during intravascular and intracardiac maneuvers, while still allowing the interventionist to monitor the position of the delivery sheath/catheter with respect to the respective intracardiac and intravascular tissues. The catheter's position will be rendered in real-time using AR HMD, granting the supervision of its position with respect to potentially critical regions of the vessels (e.g., bifurcations, calcific deposits, tortuous tracts), and allow for more intuitive manual correction of the path or of the speed of the catheter. In this regard, we developed a method to visualize with millimetric precision the position of a sensor that can be embedded in any type of catheters, sheath or probe through the use of an optical see-through HMD in a continuous and real-time manner. In particular, the proposed system was appositely designed to be independent from the operator's capability and hence robust with respect to human errors, and to be easy and quick thanks to the simple calibration procedure. Our preliminary experimental results confirmed that our registration method is effective independently from the expertise of the user accomplishing the procedure.

Moreover we quantified the accuracy of the system in the entire acquisition volume of the sensor, obtaining a quite homogeneous distribution of the error. The accuracy of the alignment showed no dependency on the position of the sensor with respect to the magnetic field generator or on other factors that could influence the precision of the system and then its usability, resulting in an average error of 2.70 ± 0.36 mm and 2.68 ± 0.79 mm respectively for intra- and

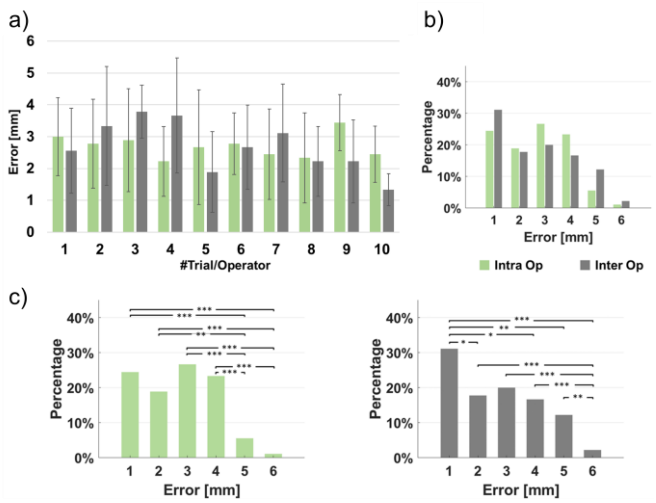


Fig. 8. a) Bar graphs showing the median values and interquartile range of the calibration error over all the nine positions in the acquisition volume in 10 different evaluation tests; b) comparison between the frequency of occurrence of each error, in the intra- and inter-operative scenario; c) frequency of occurrence – for all the 10 tests – of the errors. The level of significance of their statistical comparison is indicated with '*'. The figure represents intra- and inter-operator results respectively in green and gray.

inter-operator measurements. About 70% among all the measured errors were below 3 mm, while 31% of the inter-operator error measurements were found to be in the smallest, most centered sphere corresponding to an error equal or less than 1 mm. In this regard it is worth noting that all the observations done by the users are affected by an overestimation of the error: for the sake of simplicity and feasibility of the evaluation procedure, the sensor falling in one of the spheres was deemed to have an error corresponding to the external radius of that sphere, while in reality its error could have been intermediate between the radius of the immediately smaller sphere and the considered external radius (for example if the sensor's tip was in the fourth yellow sphere, see Fig. 6b, it was considered to have a 4 mm error, while in reality its error could have been between 3 mm and 4 mm). The same consideration applies to those points perfectly aligned with the center (small red sphere) for which an error of 1 mm was considered instead of a precise value ranging from 0 to 1 mm. This is a direct consequence of the fact that the alignment can be perceived only by the user's eye, letting the measurements of the registration be a challenging task. In this study we then have proposed an evaluation method that can give quantitative results based on the qualitative observation of multiple spheres with a known size. Due to the still existent limitation of all the commercial HMDs in visualizing sub-millimetric objects, mostly when they are positioned close to the user's eyes, the choice to overestimate the error, rounding up all the obtained values, was deemed the safest one. Other studies described a similar setup for navigation purposes using optical see-through HMD, exploiting both the first and second version of the HoloLens commercial device, coupled with an EM system. As stated in the introduction, Kuhlemann et al. [11] first showed the feasibility of a system aimed at radiation-free endovascular interventions, proposing however a calibration procedure that relies on manually picking holographic landmarks with an EM pointing device. As they reported, this method introduced inaccuracies in the overall system. Moreover, they did not quantify at all the accuracy of the registration between the virtual and the real sensorized catheter, as they considered this to be a separate procedure that requires the development of a specific and dedicated validation method. Similarly, Garcia-Vazquez et al. [12] presented a method for performing endovascular aortic repair (EVAR) using both HoloLens1 and an EM device, showing the feasibility of such a procedure, but without presenting objective data endpoints nor quantitative results about the registration procedure. Even if applied in a completely different clinical scenario, Tu et al. [13] described a registration procedure based on the manual alignment of a 3D printed cube, in which an EM sensor was embedded, to match 4 holographic points in the space simultaneously. The registration showed an error of 1.55 ± 0.27 mm, 1.71 ± 0.40 mm and 2.84 ± 0.78 mm respectively for the x, y, and z axis, the latter representing the depth coordinate with respect to the user's eyes. Despite the promising results, which nevertheless are in line with what we demonstrate in the present study, the registration and evaluation trials were performed only by one surgeon with extensive experience in AR-based surgical navigation. It is important to stress that a wrong depth perception during the initial alignment of the cube to the holographic environment, a personal ability that improves however with the constant use of such AR devices, could lead to a greater error in the entire registration. A dependency on the expertise of the user, or on multiple users, was not assessed. Instead, in the present study we preliminarily quantified the impact of the learning curve by assessing the intra-operator variability of the calibration procedure over 10 procedures, and we assessed the impact of inexperience in the use of the AR technology and in the calibration procedure by assessing the inter-operator variability over non-expert operators.

## V. Conclusion

To the best of our knowledge this is the first study that proposes a user-independent procedure for calibrating an HMD with an EM system presenting a quantitative evaluation between intra- and inter-operators within the entire acquisition volume of the EM system. Moreover, it represents the first study that uses the capability of HoloLens2 to automatically recognize and localize a QRcode in space and to accurately register a virtual coordinate system on a physical one. This study could therefore be of great impact in providing a proof of concept regarding how QRcode tracking works for all those studies that until now have used other image tracking systems based on external libraries (e.g., Vuforia). Our future works will focus on integrating the sensor and holographic visualization on the robotic catheters drivers to test the feasibility and accuracy of the whole system. Moreover, a registration procedure to align an holographic anatomical model on the patient will be integrated to give the surgeon a more realistic visual feedback on the position of the catheters compared to the anatomical structures.

## References

[1] H. C. Herrmann *et al.*, "Effect of percutaneous mitral repair with the MitraClip device on mitral valve area and gradient.," *EuroIntervention*, vol. 4,

no. 4, pp. 437–42, Jan. 2009, doi: 10.4244/eijv4i4a76.

[2] S. J. Baron *et al.*, "Cost-Effectiveness of Transcatheter Mitral Valve Repair Versus Medical Therapy in Patients with Heart Failure and Secondary Mitral Regurgitation: Results from the COAPT Trial," *Circulation*, vol. 140, no. 23, pp. 1881–1891, 2019, doi: 10.1161/CIRCULATIONAHA.119.043275.

[3] I. Mahdjoub *et al.*, "Is the MitraClip® procedure profitable in a high-volume French hospital?," *Arch. Cardiovasc. Dis.*, vol. 112, no. 11, pp. 691–698, Nov. 2019, doi: 10.1016/j.acvd.2019.07.002.

[4] P. Legeza, G. W. Britz, T. Loh, and A. Lumsden, "Current utilization and future directions of robotic-assisted endovascular surgery.," *Expert Rev. Med. Devices*, vol. 17, no. 9, pp. 919–927, Sep. 2020, doi: 10.1080/17434440.2020.1814742.

[5] "ARTERY website." https://www.artery-project.eu/.

[6] H. Iqbal, F. Tatti, and F. Rodriguez y Baena, "Augmented reality in robotic assisted orthopaedic surgery: A pilot study," *J. Biomed. Inform.*, vol. 120, no. June, p. 103841, 2021, doi: 10.1016/j.jbi.2021.103841.

[7] L. Qian, A. Deguet, and P. Kazanzides, "ARssist: Augmented reality on a head-mounted display for the first assistant in robotic surgery," *Healthc. Technol. Lett.*, vol. 5, no. 5, pp. 194–200, 2018, doi: 10.1049/htl.2018.5065.

[8] L. Qian *et al.*, "FlexiVision: Teleporting the surgeon's eyes via robotic flexible endoscope and head-mounted display," *IEEE Int. Conf. Intell. Robot. Syst.*, pp. 3281–3287, 2020, doi: 10.1109/IROS45743.2020.9340716.

[9] E. Lugez, H. Sadjadi, D. R. Pichora, R. E. Ellis, S. G. Akl, and G. Fichtinger, "Electromagnetic tracking in surgical and interventional environments: usability study," *Int. J. Comput. Assist. Radiol. Surg.*, vol. 10, no. 3, pp. 253–262, 2015, doi: 10.1007/s11548-014-1110-0.

[10] K. O'donoghue, H. A. Jaeger, and P. Cantillon-Murphy, "A radiolucent electromagnetic tracking system for use with intraoperative x-ray imaging," *Sensors*, vol. 21, no. 10, 2021, doi: 10.3390/s21103357.

[11] I. Kuhlemann, M. Kleemann, P. Jauer, A. Schweikard, and F. Ernst, "Towards X-ray free endovascular interventions - Using HoloLens for on-line holographic visualisation," *Healthc. Technol. Lett.*, vol. 4, no. 5, pp. 184–187, 2017, doi: 10.1049/htl.2017.0061.

[12] V. Garciá-Vázquez *et al.*, "Navigation and visualisation with HoloLens in endovascular aortic repair," *Innov. Surg. Sci.*, vol. 3, no. 3, pp. 167–177, 2020, doi: 10.1515/iss-2018-2001.

[13] P. Tu, Y. Gao, A. J. Lungu, D. Li, H. Wang, and X. Chen, "Augmented reality based navigation for distal interlocking of intramedullary nails utilizing Microsoft HoloLens 2," *Computers in Biology and Medicine*, vol. 133. 2021, doi: 10.1016/j.compbiomed.2021.104402.

[14] L. Qian *et al.*, "Comparison of optical see-through head-mounted displays for surgical interventions with object-anchored 2D-display," 2018, doi: 10.1007/s11548-017-1564-y.Comparison.

[15] S. Thompson *et al.*, "SciKit-Surgery: compact libraries for surgical navigation," *Int. J. Comput. Assist. Radiol. Surg.*, vol. 15, no. 7, pp. 1075–1084, 2020, doi: 10.1007/s11548-020-02180-5.

[16] S. D. B. K. S. Arun, T.S. Huang, "Least-Squares Fitting of Two 3-D Points Sets," *IEEE Trans. Pattern Anal. Mach. Intell.*, no. 5, pp. 698–700, 1987.

[17] M. J. Mack *et al.*, "Transcatheter Aortic-Valve Replacement with a Balloon-Expandable Valve in Low-Risk Patients," *N. Engl. J. Med.*, vol. 380, no. 18, pp. 1695–1705, May 2019, doi: 10.1056/NEJMoa1814052.

[18] I. Al Amri, F. van der Kley, M. J. Schalij, N. Ajmone Marsan, and V. Delgado, "Transcatheter mitral valve repair therapies for primary and secondary mitral regurgitation," *Future Cardiol.*, vol. 11, no. 2, pp. 153–169, Mar. 2015, doi: 10.2217/fca.15.8.

[19] H. Rafii-Tari, C. J. Payne, and G.-Z. Yang, "Current and emerging robot-assisted endovascular catheterization technologies: a review.," *Ann. Biomed. Eng.*, vol. 42, no. 4, pp. 697–715, Apr. 2014, doi: 10.1007/s10439-013-0946-8.